Journal of The Electrochemical Society, **157** (3) A333-A339 (2010)
0013-4651/2010/157(3)/A333/7/$28.00 © The Electrochemical Society

Synthesis, Characterization, and Electrochemical Properties of $LiCr_xNi_yMn_{2-x-y}O_4$ Spinels as Cathode Material for 5 V Lithium Battery

S. Rajakumar, R. Thirunakaran, A. Sivashanmugam, and S. Gopukumar[z]

Central Electrochemical Research Institute (Council of Scientific and Industrial Research), Karaikudi, Tamil Nadu 630 006, India

Sol–gel assisted spinel $LiCr_xNi_yMn_{2-x-y}O_4$ ($0 \le x \le 0.4$ and $0 \le y \le 0.4$) has been synthesized. The thermal study of the precursor was carried out by thermogravimetric and differential thermal analyses. Furthermore, the material has been subjected to X-ray diffraction, scanning electron microscopy, Fourier transform IR spectroscopy analysis, X-ray photoelectron spectroscopy, cyclic voltammetry studies, and electrochemical charge–discharge studies. The X-ray diffraction of $LiCr_xNi_yMn_{2-x-y}O_4$ matches well with the Joint Committee on Powder Diffraction Standard card no. 35-782, confirming the formation of a single-phase spinel. Charge–discharge studies were carried out between 3 and 5 V to understand the electrochemical behavior of the undoped and doped spinels. $LiCr_{0.25}Ni_{0.25}Mn_{1.5}O_4$ calcined at 850°C possesses a particle size of around 70 nm and exhibits an initial discharge capacity of 105 mAh g^{-1} stabilizing at 98 mAh g^{-1} over the investigated 20 cycles. However, maleic acid derived $LiCr_{0.25}Ni_{0.25}Mn_{1.5}O_4$ delivers a stable higher discharge capacity of ~115 mAh g^{-1} over the investigated 20 cycles and is a promising 5 V cathode material.
 [DOI: 10.1149/1.3283015]

Manuscript submitted August 25, 2009; revised manuscript received November 5, 2009. Published February 1, 2010.

The technological escalation in the microelectronics zone and the onset of applications ranging from toys to missiles necessitate low cost, environment-friendly, and thermally stable lithium batteries with high power and energy densities. To meet these requirements, intense research has been focused on the spinel $LiMn_2O_4$ as a prospective cathode material in lithium secondary batteries due to its low toxicity, easy availability, environment-friendly nature, the facile synthesis of this phase, and also the low cost of lithium manganese oxide compared to other transition-metal oxides such as $LiCoO_2$ and $LiNiO_2$.[1,2] Recent trends in lithium batteries have been focused on the development and characterization of an enhanced performing high voltage cathode material operating in the 5 V regions.[3] Researchers revealed that partial substitution of manganese in $LiMn_2O_4$ with 3d transition metals renders it a high voltage material with improved cyclability. Extending this concept of replacing Mn atoms by 3d transition-metal atoms in $LiMn_2O_4$, Zhang et al.[4] substituted Cr, whereas Amdouni et al.[5] and Wu et al.[6] substituted Ni in $LiM_xMn_{2-x}O_4$ (M = Cr, Ni) and concluded that the lost capacity at the 4 V plateau reappears in the higher voltage plateau (>4.5 V for M = Cr and >4.7 for M = Ni).[7,8] Several papers reported that single-/multidoped cubic spinels and layered compounds were charged up to 5 V to increase the capacity and reduce the capacity fade upon repeated cycling.[9-11]

The Ni substitution leads to higher discharge plateaus around 5 V and, in turn, to a high power density. The structural disintegration upon cycling can be prevented by substituting metal with a higher bonding energy. Toward this goal, Cr is substituted to maintain the spinel structure during cycling as the bonding energy of Cr–O is stronger than that of Mn–O and Ni–O.[12]

In this present study, $LiCr_xNi_yMn_{2-x-y}O_4$ ($0 \le x \le 0.4$ and $0 \le y \le 0.4$) using glycine or maleic acid as chelating agents has been synthesized by a sol–gel technique. The physical and electrochemical studies of the synthesized material have been done, and the experimental results are discussed.

Experimental

Figure 1 shows the flow chart for the synthesis of $LiCr_xNi_yMn_{2-x-y}O_4$ by a sol–gel method using glycine or maleic acid as chelating agents. Stoichiometric amounts of nitrates of lithium, manganese, chromium, and nickel were uniformly mixed and dissolved in triple-distilled water. This solution was continuously stirred for some time with mild heating to obtain a homogeneous solution. The solution was added drop by drop into an aqueous solution of 3 M glycine or 1 M maleic acid solution, which is used as chelating agent. The pH of the solution was adjusted between 5 and 7.5 using ammonia solution. The process of stirring and heating was continued until a solid gel was obtained. Furthermore, the gel was initially heated overnight at 110°C. The thermal behavior of the gel precursors was characterized by thermogravimetry (TG) and differential thermal analysis (DTA) in a PL Thermal Sciences Instrument model STA 1500. All experiments were carried out in air at a heating ramp of 20°C/min with typically 50 mg samples. Furthermore, this gel mass was calcined at different temperatures, viz., 250, 400, 600, and 850°C for 8 h in alumina crucibles. The resulting calcined samples are physically characterized using an X-ray diffractometer (XRD, JEOL 8030) with nickel filtered Cu Kα radiation, a scanning electron microscope (SEM, Hitachi S-3000 H), a Fourier transform infrared (FTIR) spectroscope (Perkin-Elmer, model paragon-500 spectrophotometer), and an X-ray photoelectron spectroscope (XPS, VG electron spectroscope X-ray source Al Kα radiation) with a scan range of 0–1200 eV binding energy. The col-

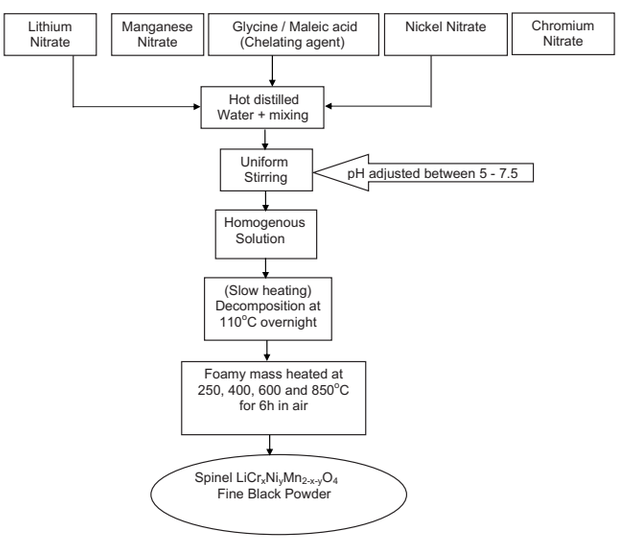

Figure 1. Flow chart for the synthesis of $LiCr_xNi_yMn_{2-x-y}O_4$ by a sol–gel method using glycine/maleic acid chelating agents.

[z] E-mail: deepika_41@rediffmail.com

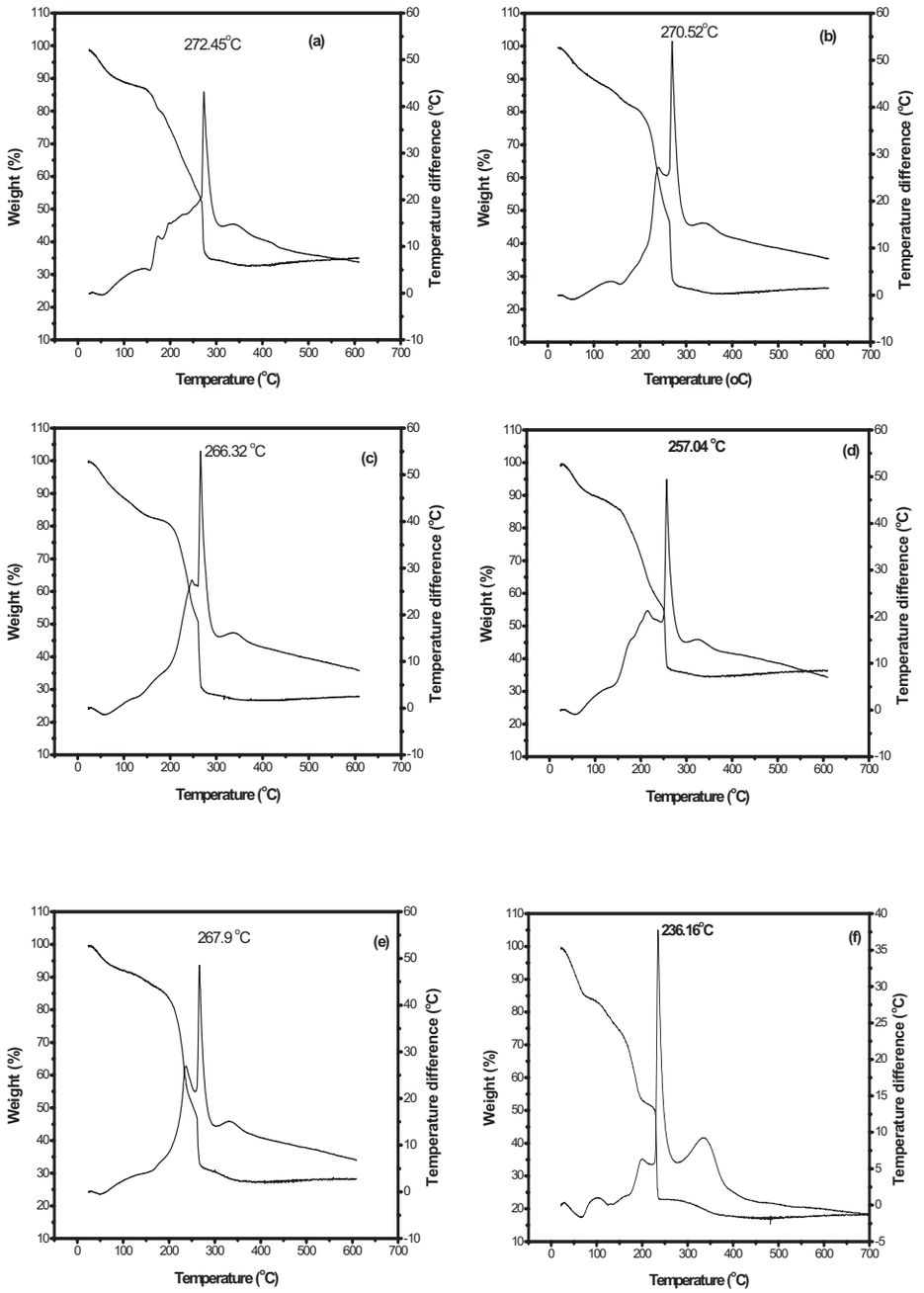

Figure 2. TG/DTA curves of the glycine assisted $LiCr_xNi_yMn_{x-y}O_4$. (a) Cr: 0.1, Ni: 0.4; (b) Cr: 0.2, Ni: 0.3; (c) Cr: 0.25, Ni: 0.25; (d) Cr: 0.3, Ni: 0.2; (e) Cr: 0.4, Ni: 0.1; and (f) Cr: 0.25, Ni: 0.25 (maleic acid assisted).

lected high resolution XPS spectra were analyzed using an XPS peak software fitting program. The energy scale was adjusted on the carbon peak in the C 1s spectra at 284.5 eV.

Electrochemical Studies

The electrochemical cell was a typical 2016-type coin cell (Hohsen Co., Japan) assembled using lithium metal as anode, Celgard 2400 as separator, 1 M solution of $LiPF_6$ in a 50:50 (v/v) mixture of ethylene carbonate/diethylene carbonate as electrolyte, and the synthesized material as cathode active material. The cathodes were prepared using a slurry coating procedure over an aluminum foil of 18 mm diameter. The slurry is an 85:10:5 mixture of the respective cathode active material, acetylene black, and poly(vinylidene fluoride) in *N*-methyl-2-pyrrolidone. A battery cycling tester unit has been employed for evaluating the charge–discharge characteristics in the voltage range (3.0–5.0 V) at the C/10 rate. Cyclic voltammetry studies of $LiCr_{0.25}Ni_{0.25}Mn_{1.5}O_4$ electrodes were performed at a scan rate of 10 $\mu V\ s^{-1}$ in the potential range of 3.0–5.0 V using a PAR 273A (EG&G) potentiostat.

Results and Discussion

Thermal studies.— Figure 2 shows the TG/DTA curves of the glycine and maleic acid assisted sol–gel derived $LiCr_xNi_yMn_{x-y}O_4$. The TG curves of all dual-doped spinel depict two weight loss zones. Ab initio, a weight loss of ~15% in $LiCr_{0.1}Ni_{0.4}Mn_{1.5}O_4$ is obtained up to 152°C and may be due to the loss of a water molecule. Subsequently, another weight loss zone is seen between 152 and 300°C corresponding to 50% weight loss, which could be ascribed to the decomposition of glycine or maleic acid as chelating agents and nitrate precursors. DTA curves show a shallow and high sharp exothermic peak, suggesting the formation of a spinel com-

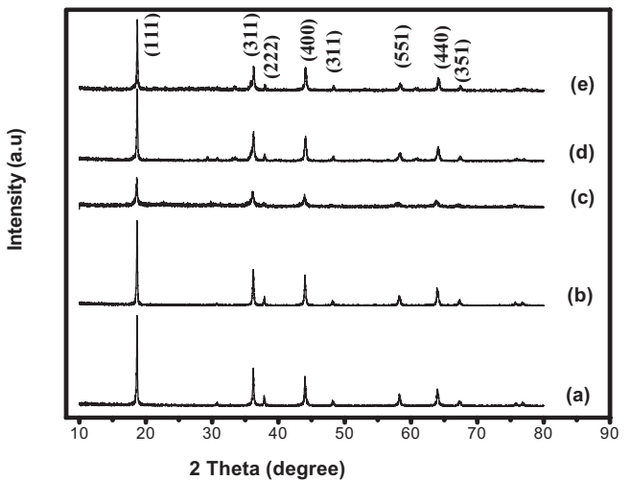

Figure 3. XRD patterns of the sol–gel derived $LiCr_xNi_yMn_{2-x-y}O_4$ calcined at 850°C. (a) Cr: 0.1, Ni: 0.4; (b) Cr: 0.2, Ni: 0.3; (c) Cr: 0.25, Ni: 0.25; (d) Cr: 0.3, Ni: 0.2; and (e) Cr: 0.4, Ni: 0.1.

pound at around 175 and 272°C. The formation temperature of $LiCr_{03}Ni_{0.2}Mn_{1.5}O_4$ is low, i.e., ~257.04°C in view of the higher specific heat of nickel (444 kJ/mol) compared to chromium (397 kJ/mol). Furthermore, the formation temperatures with two exothermic peaks at all dual-doped spinel compounds are seen between 257 and 272°C without much variation. However, in maleic acid as chelating agent, the formation temperature is much lower (236°C) and could be due to the higher combustible nature associated with

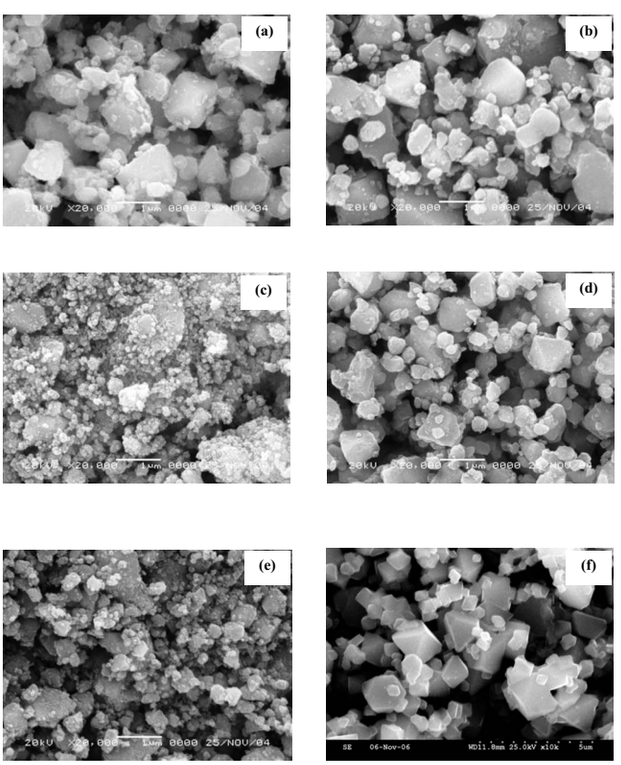

Figure 4. SEM images of different dopant levels of the glycine assisted $LiCr_xNi_yMn_{x-y}O_4$ calcined at 850°C. (a) Cr: 0.1, Ni: 0.4; (b) Cr: 0.2, Ni: 0.3; (c) Cr: 0.25, Ni: 0.25; (d) Cr: 0.3, Ni: 0.2; (e) Cr: 0.4, Ni: 0.1; and (f) Cr: 0.25, Ni: 0.25 (maleic acid assisted).

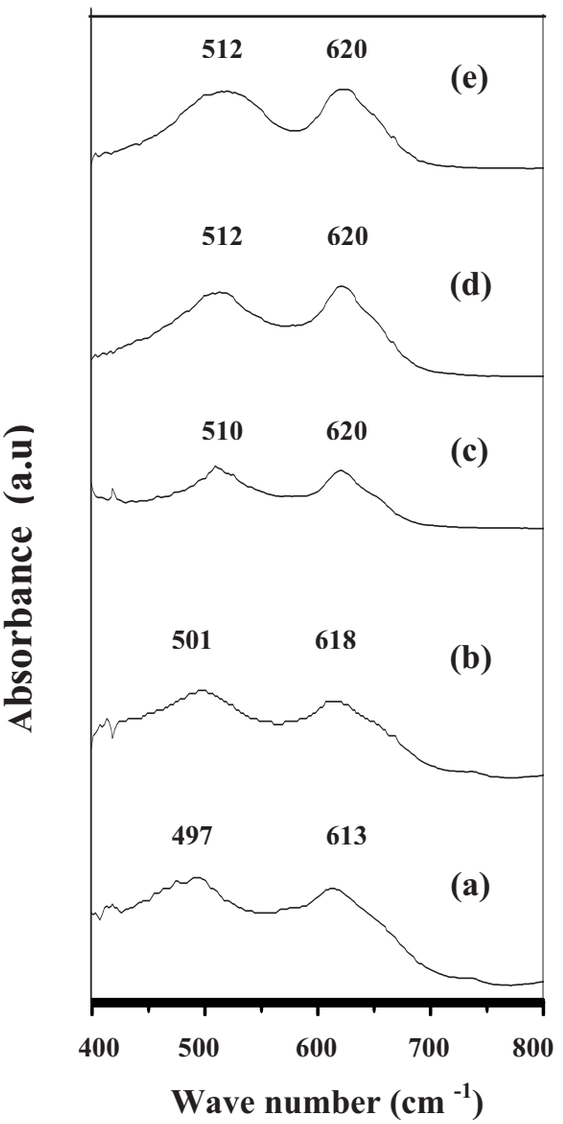

Figure 5. FTIR spectra of the glycine assisted $LiCr_xNi_yMn_{x-y}O_4$ calcined at 850°C. (a) Cr: 0.1, Ni: 0.4; (b) Cr: 0.2, Ni: 0.3; (c) Cr: 0.25, Ni: 0.25; (d) Cr: 0.3, Ni: 0.2; and (e) Cr: 0.4, Ni: 0.1.

two carboxylic acids. Finally, all the sol–gel synthesized nitrate precursors confirm no weight loss beyond ~350°C, suggesting the completion of thermal events.

XRD.— Figure 3 shows XRD patterns of the sol–gel derived $LiCr_xNi_yMn_{2-x-y}O_4$ calcined at 850°C. High intensity peaks such as (111), (311), (222), (400), (331), (551), (440), and (351) obtained from the samples calcined at 850°C show the high degree of crystallinity with the phase pure structure and with the formation of the spinel compound, which has a striking similarity with previous researchers.[13,14] The pristine spinel has the *Fd3m* space group wherein lithium occupies the 8a tetrahedral sites, manganese ions ($Mn3^+$ and Mn^{4+}) occupy the 16d sites, and O^{2-} occupies the 32e sites.[15] However, when it is heated above 900°C, some impurities in the additional peaks are observed, such as Mn_3O_4 and Li_2MnO_3. In other words, when the spinel structure is calcined to 900°C, it transforms into a layered structure of $LiMnO_2$, which is unstable below 900°C, and it is oxidized in air to form $LiMn_2O_4$.[16] All the peak

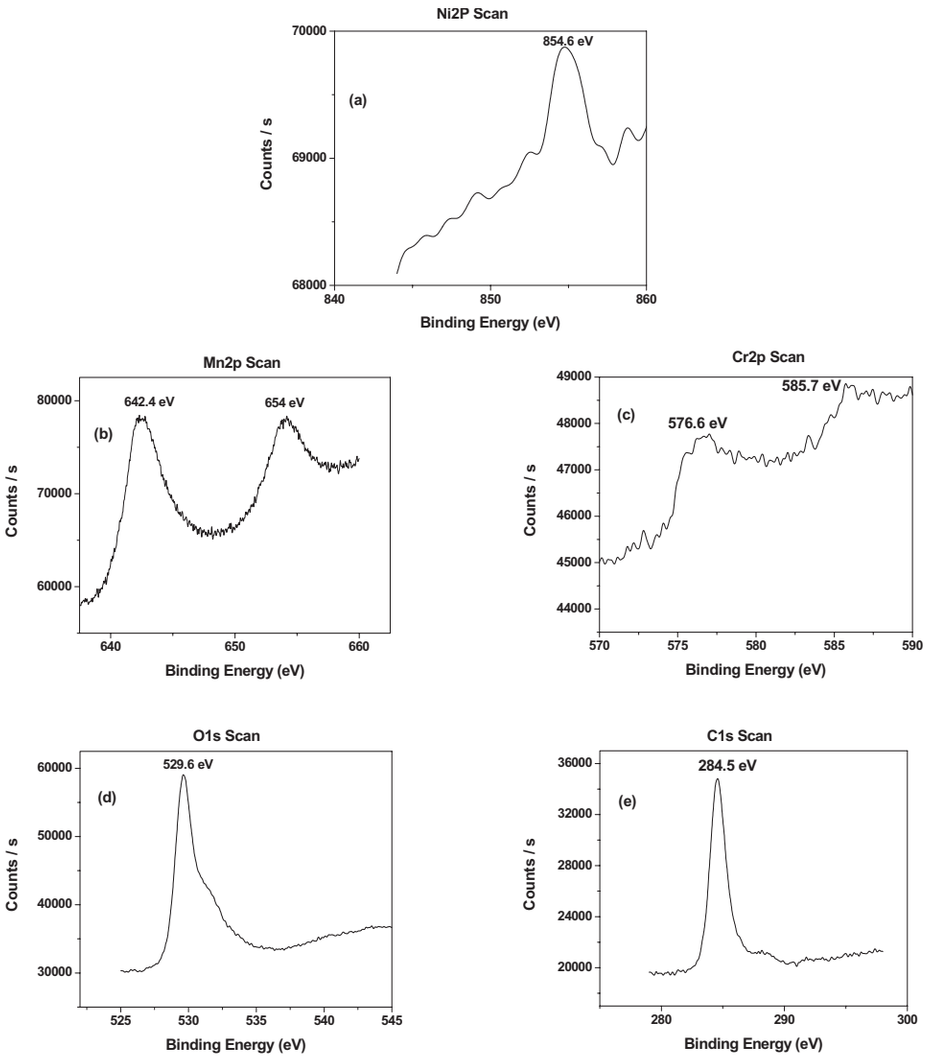

Figure 6. XPS studies of $LiCr_{0.25}Ni_{0.25}Mn_{1.5}O_4$.

signatures of the spinel agree well with JCPDS card no. 35-782. Glycine or maleic acid as chelating agent in the sol–gel synthesis is beneficial for favoring the metal ligand chain between Mn–O and COO^-, resulting in the formation of the spinel product. Finally, the highly crystalline compounds were subjected to electrochemical charge–discharge studies.

FTIR spectroscopy.— Figure 4 shows the FTIR spectra of the glycine or maleic acid assisted $LiCr_xNi_yMn_{x-y}O_4$ calcined at 850°C. The synthesized sample was ground, mixed with KBr, and pressed into 10 mm diameter pellets. The FTIR spectra reveal asymmetric stretching and asymmetric bending vibrations for the lithium manganese oxide spinel. The high frequency bands of the FTIR absorption spectrum of $LiMn_2O_4$ located at approximately 615 and 513 cm^{-1} are attributed to the asymmetric stretching modes of the MnO_6 octahedra, whereas the low frequency bands at approximately 225, 262, 355, and 420 cm^{-1} have a mixed character due to the presence of the bending modes of O–/Mn–O bonds and the modes of LiO_4 tetrahedra in the spinel structure. FTIR study on chromium- and nickel-doped spinel had been investigated by several authors.[5,17] The IR spectral band seen at a lower wavelength of around 614 cm^{-1} may be assigned to the Cr–O stretching vibration band, and another band is shown at a higher wavenumber of around 512 cm^{-1} due to Ni–O. These observations agree well with previous researchers. Furthermore, it is ascertained that there are no significant spectral reflections as all samples were calcined at 850°C except for a slight shift for the nickel dopant toward a lower wavenumber.

SEM.— Figure 5 shows SEM images of different dopant levels of the glycine or maleic acid assisted $LiCr_xNi_yMn_{x-y}O_4$ calcined at 850°C. The surface morphology of $LiCr_{0.1}Ni_{0.4}Mn_{1.5}O_4$ calcined at 850°C (Fig. 5a) clearly illustrates an average particle size of 0.5 μm, whereas in the other two doped samples ($LiCr_{0.2}Ni_{0.3}Mn_{1.5}O_4$, $LiCr_{03}Ni_{0.2}Mn_{1.5}O_4$), the average spherical grain size is around 0.5 μm. Furthermore, $LiCr_{0.4}Ni_{0.1}Mn_{1.5}O_4$ depicts a small particle size (0.3 μm) with small grains compared to other dopants. However, in the maleic acid derived $LiCr_{0.25}Ni_{0.25}Mn_{1.5}O_4$ calcined at 850°C, an average particle size of ~0.25 μm is reflected in the charge–discharge studies for obtaining high electrochemical activity and coulombic efficiency. The above preliminary observations suggest that an equal ratio of the Cr and Ni dopants ($LiCr_{0.25}Ni_{0.25}Mn_{1.5}O_4$) in the pristine spinel is beneficial for enhancing the electrochemical performance.

XPS studies.— The $LiCr_{0.25}Ni_{0.25}Mn_{1.5}O_4$ sample has been analyzed to divulge the oxidation states of the metal genus present in the spinel compound (shown in Fig. 6a-c). The Ni $2p_{3/2}$ XPS spectrum is located at 854.6 eV, and it has been assigned to Ni^{2+}. The satellite peak at 858.7 eV has been assigned to multiple splitting of

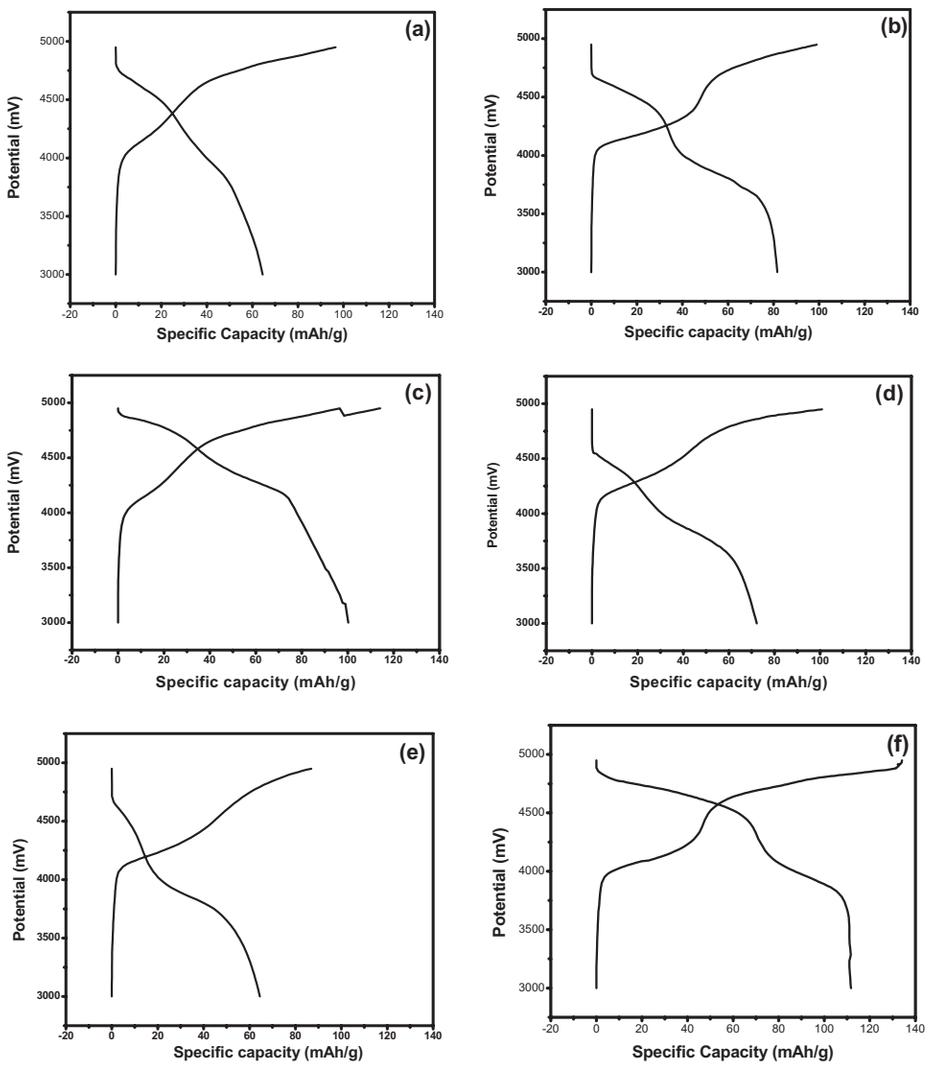

Figure 7. Charge–discharge behavior of different dopant levels of the glycine assisted $LiCr_xNi_yMn_{x-y}O_4$ calcined at 850°C. (a) Cr: 0.1, Ni: 0.4; (b) Cr: 0.2, Ni: 0.3; (c) Cr: 0.25, Ni: 0.25; (d) Cr: 0.3, Ni: 0.2; (e) Cr: 0.4, Ni: 0.1; and (f) Cr: 0.25, Ni: 0.25 (maleic acid assisted).

nickel oxide energy levels. The peaks closely agree with those reported by earlier researchers.[9,18,19] In Fig. 6b, the binding energy major peak value is due to Mn $2p_{3/2}$, and the satellite peaks are at 642.4 and 654 eV. The binding energy major peak value is a bit higher than those reported, and it could be assigned due to the increased content in Mn^{4+} of the spinels, as derived from the average oxidation states by suppressing Mn^{3+}.[20,21] In the Cr 2p scan (Fig. 6c), the binding energy is located at 576.6 and 585.7 eV, is assigned to Cr^{3+}, and agrees well with literature.[22] The binding energy peaks observed at 529.6 and 284.5 eV are for O 1s and C 1s.

Galvanostatic charge–discharge and cycling studies.— Figure 7a-e shows the first charge–discharge behavior of different dopant levels of the glycine assisted $LiCr_xNi_yMn_{x-y}O_4$ calcined at 850°C. The $LiCr_{0.1}Ni_{0.4}Mn_{1.5}O_4$ compound calcined at 850°C delivered a discharge capacity of 64 mAh g^{-1} against a charging capacity of 95 mAh g^{-1} corresponding to 75% coulombic efficiency. It is evident that all other cells comprising the cathode materials, viz., $LiCr_{0.2}Ni_{0.3}Mn_{1.5}O_4$, $LiCr_{0.25}Ni_{0.25}Mn_{1.5}O_4$, $LiCr_{03}Ni_{0.2}Mn_{1.5}O_4$, and $LiCr_{0.4}Ni_{0.1}Mn_{1.5}O_4$, first deliver discharge capacities of ~82, 100, 72, and 65 mAh g^{-1}, respectively. Among all the investigated cells, the equal ratio of dopants in $LiCr_{0.25}Ni_{0.25}Mn_{1.5}O_4$ with glycine as chelating agent exhibits better electrochemical performance (~100 mAh g^{-1}) with a high coulombic efficiency of ~85%.

The higher first charge–discharge (~115 mAh g^{-1}) is obtained in the maleic acid assisted synthesis of $LiCr_{0.25}Ni_{0.25}Mn_{1.5}O_4$ calcined at 850°C (Fig. 7f). This observation could be assigned to the two COOH groups present in maleic acid compared to one in glycine, thereby facilitating the formation of metal ligand chains between Mn–O and two $COOH^-$ groups, resulting in the formation of submicrometer-sized particles and resulting in stabilizing the spinel structure. However, at unequal dopant concentrations, there are much decrease in discharge capacities, owing to the high density of the cation distribution.

Figure 8a-e illustrates the cycling behavior of the investigated 20 cycles and the corresponding coulombic efficiencies for different dopant levels of the glycine assisted $LiCr_xNi_yMn_{x-y}O_4$ calcined at 850°C. The $LiCr_{0.1}Ni_{0.4}Mn_{1.5}O_4$ compound calcined at 850°C shows an initial discharge capacity of 64 mAh g^{-1}, but the capacity drastically fades up to 10 cycles and finally stabilizes at around 45 mAh g^{-1} over the investigated 20 cycles. In $LiCr_{0.2}Ni_{0.3}Mn_{1.5}O_4$, a very low capacity fade has been observed, i.e., 0.01 mAh g^{-1} $cycle^{-1}$, vindicating the better capacity retention with a discharge capacity of 81 mAh g^{-1} corresponding to a coulombic efficiency of 85%. Furthermore, in the other two compositions ($LiCr_{03}Ni_{0.2}Mn_{1.5}O_4$ and $LiCr_{0.4}Ni_{0.1}Mn_{1.5}O_4$), the discharge capacities of 75 and 65 mAh g^{-1}, respectively, are delivered in the 20th cycle, corresponding to a capacity fade of 0.12 and 0.04 mAh g^{-1} $cycle^{-1}$ with a coulombic efficiency of ~85%. The

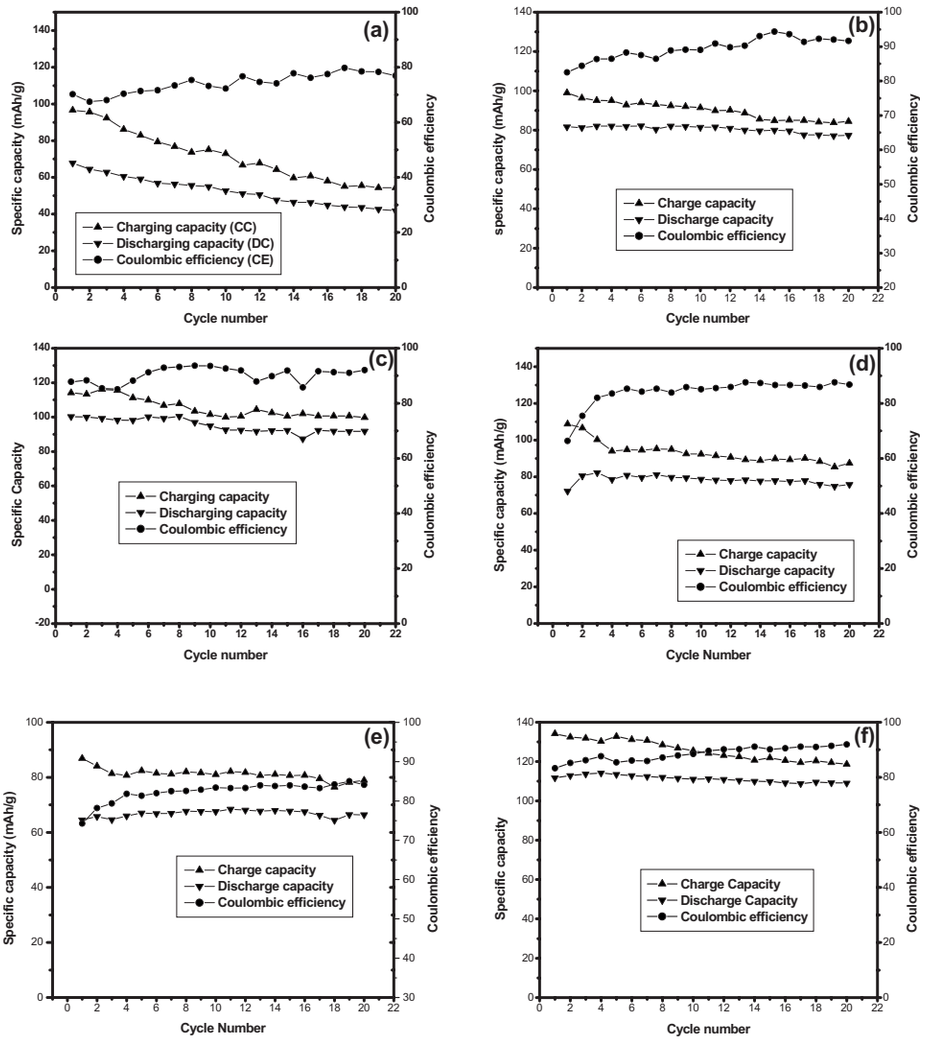

Figure 8. Cycling behavior of different dopant levels of the glycine assisted $LiCr_xNi_yMn_{x-y}O_4$ calcined at 850°C. (a) Cr: 0.1, Ni: 0.4; (b) Cr: 0.2, Ni: 0.3; (c) Cr: 0.25, Ni: 0.25; (d) Cr: 0.3, Ni: 0.2; (e) Cr: 0.4, Ni: 0.1; and (f) Cr: 0.25, Ni: 0.25 (maleic acid assisted).

equal doping ratio of $LiCr_{0.25}Ni_{0.25}Mn_{1.5}O_4$ with maleic acid as chelating agent delivers the maximum capacity of ~115 mAh g^{-1} with a capacity fade of only 0.01 mAh g^{-1} $cycle^{-1}$, corresponding to a coulombic efficiency of 92%, and exhibits a higher capacity with a very low capacity fade than glycine assisted spinel. The observations indicate that the equal doping ratio of $LiCr_{0.25}Ni_{0.25}Mn_{1.5}O_4$ with maleic acid as chelating agent exhibits a higher discharge capacity and a good coulombic efficiency compared to other doped spinels using glycine.

$LiCr_{0.1}Ni_{0.4}Mn_{1.5}O_4$ was reported recently by Liu et al.[12] using citric acid as chelating agent to obtain a high discharge capacity of the spinel. In his paper, only one composition, i.e., $LiCr_{0.1}Ni_{0.4}Mn_{1.5}O_4$, synthesized by a sol–gel method having a low concentration of chromium and a high concentration of nickel, delivered a discharge capacity of ~110 mAh g^{-1}. Furthermore, Sun et al. reported the electrochemical performance of $LiCr_{0.4}Ni_{0.2}Mn_{1.4}O_4$ obtained by a solution method after heating for 18 h to use as a cathode material for lithium rechargeable batteries.[7] In our present study, an attempt has been made to use either glycine or maleic acid as chelating agent so as to enhance the electrochemical performance of the spinel. However, our results are superior with maleic acid assisted manganese spinel ($LiCr_{0.25}Ni_{0.25}Mn_{1.5}O_4$) exhibits a very stable discharge capacity of ~115 mAh g^{-1} with a very low capacity fade 0.01 mAh g^{-1} $cycle^{-1}$ up to 20 cycles.

Cyclic voltammetry studies.— Figure 9 depicts the typical cyclic voltammetric curve obtained from $LiCr_{0.25}Ni_{0.25}Mn_{1.5}O_4$. There are no peaks around the 3 V region, revealing the absence of Mn^{3+}, which is present in the sample and is corroborated by the Mn 2p scan of the XPS studies. There are two major oxidation peaks at around 4.2 and 4.9 V, and two major reduction peaks are observed at around 3.9 and 4.6 V, which can be attributed to the lithium deintercalation and reintercalation processes. These peaks are also signatures of the cubic spinel compounds and indicate perfect reversibility. The peaks at around 4.2 V could be assigned to the electrochemical oxidation of manganese ions, and the peaks at around 4.9 V could be assigned to the oxidation of Ni and Cr. The reduction processes of Mn, Ni, and Cr are indicated by the two reduction peaks observed at 3.9 and 4.6 V.

Conclusions

$LiCr_xNi_yMn_{2-x-y}O_4$ ($0 \le x \le 0.4$ and $0 \le y \le 0.4$) has been synthesized using either glycine or maleic acid via a sol–gel method to obtain submicrometer-sized particles to enhance the electrochemical stability of the spinel. The XRD and SEM studies show the formation of a single-phase compound with spherical grains of the surface morphology having an average particle size of 0.5 μm. The synthesized spinel has been ascertained by the XRD and FTIR studies. Charge–discharge studies confirm that among all the investi-

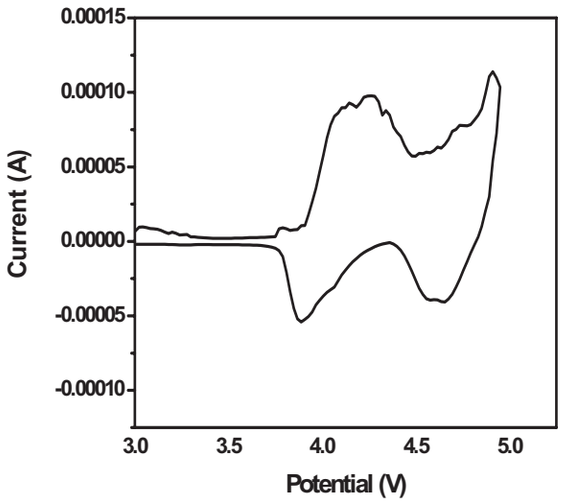

Figure 9. Cyclic voltammetry studies of $LiCr_{0.25}Ni_{0.25}Mn_{1.5}O_4$.

gated cells, the equal ratio of the dopants with maleic acid assisted $LiCr_{0.25}Ni_{0.25}Mn_{1.5}O_4$ exhibits a maximum superior performance ($\sim$115 mAh g^{-1}) with a capacity fade of 0.01 mAh g^{-1} $cycle^{-1}$ corresponding to a coulombic efficiency of 92% compared to that of glycine assisted $LiCr_{0.25}Ni_{0.25}Mn_{1.5}O_4$ in the investigated 20 cycles. Finally, $LiCr_{0.25}Ni_{0.25}Mn_{1.5}O_4$ with maleic acid as chelating agent seems to be an apt positive material to deliver a high capacity for use in lithium rechargeable batteries. Furthermore, $LiCr_{0.25}Ni_{0.25}Mn_{1.5}O_4$ can be rewritten as $Li^{+1}[Cr_{0.25}]^{+3}[Ni_{0.25}]^{+2}[Mn_{0.25}]^{+3}[Mn_{1.25}]^{+4}[O_4]^{-2}$, i.e., $Li(Cr_{1/4}Ni_{1/4}Mn_{1/4})Mn_{1.25}O_4$. This is akin to $LiNi_{1/3}Co_{1/3}Mn_{1/3}O_2$, which has been recently claimed as a promising cathode material and a possible alternative to $LiCoO_2$.

Acknowledgments

The authors thank DST India for support under the DST-JST project no. JAP/SCP-011.

References

1. A. K. Shukla and T. Prem Kumar, *Curr. Sci.*, **94**, 314 (2008).
2. J. H. Kim, C. S. Yoon, and Y. K. Sun, *Electrochem. Solid-State Lett.*, **7**, A216 (2004).
3. T. Ohzuku, S. Takeda, and M. Iwanaga, *J. Power Sources*, **81-82**, 90 (1999).
4. D. Zhang, B. N. Popov, and R. E. White, *J. Power Sources*, **76**, 81 (1998).
5. N. Amdouni, K. Zaghib, F. Gendron, A. Mauger, and C. M. Julien, *Ionics*, **12**, 117 (2006).
6. H. M. Wu, J. P. Tu, X. T. Chen, D. Q. Shi, X. B. Zhao, and G. S. Cao, *Electrochim. Acta*, **51**, 4148 (2006).
7. Y. Sun, Z. Wang, X. Huang, and L. Chen, *J. Power Sources*, **132**, 161 (2004).
8. G. T. Fey, C. Z. Lu, and T. Prem Kumar, *J. Power Sources*, **115**, 332 (2003).
9. S. Rajakumar, R. Thirunakaran, A. Sivashanmugam, J. Yamaki, and S. Gopukumar, *J. Electrochem. Soc.*, **156**, A246 (2009).
10. C. N. Zaheena, C. Nithya, R. Thirunakaran, A. Sivashanmugam, and S. Gopukumar, *Electrochim. Acta*, **54**, 2877 (2009).
11. R. Thirunakaran, A. Sivashanmugam, S. Gopukumar, and R. Rajalakshmi, *J. Power Sources*, **187**, 565 (2009).
12. G. Liu, H. Xie, L. Liu, X. Kang, Y. Tian, and Y. Zhai, *Mater. Res. Bull.*, **42**, 1955 (2007).
13. R. Thirunakaran, A. Sivashanmugam, S. Gopukumar, C. W. Dunnill, and D. H. Gregory, *Mater. Res. Bull.*, **43**, 2129 (2008).
14. R. Thirunakaran, K. T. Kim, Y. M. Kang, C. Y. Seo, and J. Y. Lee, *Mater. Res. Bull.*, **40**, 177 (2005).
15. H. Yan, X. Huang, Z. Lu, H. Huang, R. Xue, and L. Chen, *J. Power Sources*, **68**, 530 (1997).
16. J. M. Tarascon, W. R. Mckinnon, F. Coowar, T. N. Bowmer, G. Amatucci, and D. Guyomard, *J. Electrochem. Soc.*, **141**, 1421 (1994).
17. C. Wu, Z. Wang, F. Wu, L. Chen, and X. Huang, *Solid State Ionics*, **144**, 277 (2001).
18. Y. Wei, K. W. Nam, K. B. Kim, and G. Chen, *Solid State Ionics*, **177**, 29 (2006).
19. S. Gopukumar, K. Y. Chung, and K. B. Kim, *Electrochim. Acta*, **49**, 803 (2004).
20. L. Hernán, J. Morales, L. Sánchez, E. Rodríguez Castellón, and M. A. G. Aranda, *J. Mater. Chem.*, **12**, 734 (2002).
21. J. C. Arrebola, A. Caballero, L. Hernan, M. Melero, J. Morales, and E. R. Castellon, *J. Power Sources*, **162**, 606 (2006).
22. M. Aronniemi, J. Sainio, and J. Lahtinen, *Surf. Sci.*, **578**, 108 (2005).